Indian J Microbiol (July–Sept 2019) 59(3):273–287
https://doi.org/10.1007/s12088-019-00801-5

ORIGINAL RESEARCH ARTICLE

Effective Inhibition of Phytopathogenic Microbes by Eco-Friendly Leaf Extract Mediated Silver Nanoparticles (AgNPs)

Mahvash Haroon[1] · Almas Zaidi[1] · Bilal Ahmed[1] · Asfa Rizvi[1] · Mohammad Saghir Khan[1] · Javed Musarrat[1,2]

Received: 13 February 2019 / Accepted: 20 March 2019 / Published online: 29 March 2019

Abstract This study was aimed at producing the eco-friendly, safe, and inexpensive silver (Ag) nanoparticles (NPs) and assessing its antimicrobial activity. Fungal pathogens isolated from diseased leaves and fruits of brinjal and bacterial pathogen obtained from a culture collection were used in this study. Green synthesis of AgNPs was performed and optimized using *Azadirachta indica* leaf extract. The newly synthesized AgNPs (λ_{max} = 437 nm) showed isotropism in size (crystal size/diameter: 21/29 ± 5 nm) and morphology under transmission and scanning electron microscopy and energy dispersive X-ray analysis. The fourier transform infrared spectroscopy data suggested the role of various aliphatic/aromatic moieties and proteins in AgNPs stabilization. The AgNPs reduced the growth of *Penicillium* sp. maximally by 92% after 6 days. The sensitivity of test fungi towards AgNPs followed the order: *Penicillium* sp. (92%) > *Fusarium* sp. (89%) > *Aspergillus* sp. (69%). Exposure of *Ralstonia solanacearum* to AgNPs (MIC/MBC 200/400 μg ml^{-1}) displayed damaged cellular envelopes, bulging of cells, and pit formation. The nucleic acid discharge showed a progressive increase from 8 to 34% (r^2 = 0.97). The cellular metabolic activity and surface adhering ability of *R. solanacearum* were completely lost at 400 μgAgNPs ml^{-1}. Results suggested that the AgNPs synthesized in this study had enough anti-pathogenic potential and could inexpensively and safely be used as a promising alternative to agrochemicals. Moreover, the findings observed in this study is likely to serve as an important indicator for the development of effective nano-control agents which in effect would help to manage some deadly phyto-pathogens capable of causing heavy losses to agricultural production systems.

Graphical Abstract Effective inhibition of phytopathogenic microbes by eco-friendly neem leaf extract mediated silver nanoparticles (AgNPs)

Electronic supplementary material The online version of this article (https://doi.org/10.1007/s12088-019-00801-5) contains supplementary material, which is available to authorized users.

✉ Bilal Ahmed
bilalahmed.amu@gmail.com

[1] Department of Agricultural Microbiology, Faculty of Agriculture Sciences, Aligarh Muslim University, Aligarh, India

[2] Present Address: School of Biosciences and Biodiversity, Baba Ghulam Shah Badshah University, Rajouri, Jammu and Kashmir, India

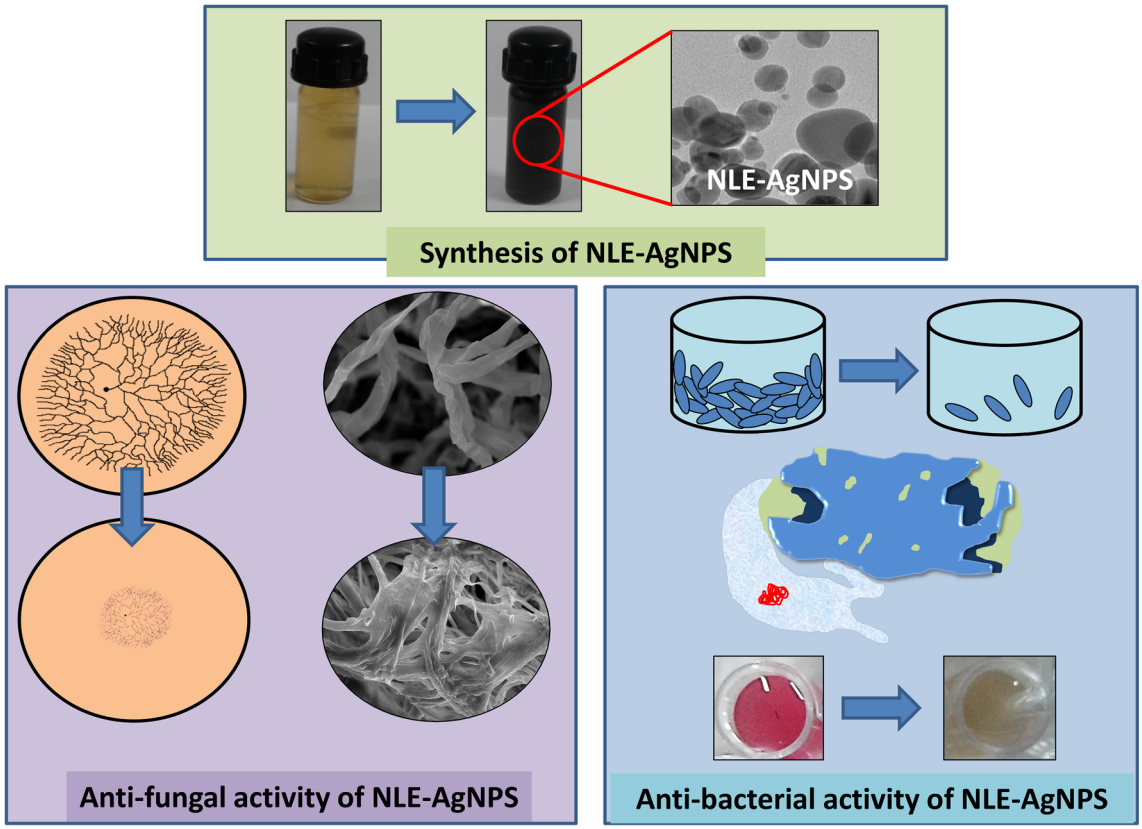

Keywords Green synthesis · *A. indica* leaf extract · Antifungal · Antibacterial · Silver nanoparticles · Plant pathogens

Introduction

Globally, the agricultural crop production is declining consistently due to many reasons; chief among them is the diseases to plants caused by numerous soil borne phytopathogens including bacteria and fungi [1]. The most common fungal pathogens are *Fusarium*, *Aspergillus*, *Penicillium*, *Rhizoctonia*, *Alternaria, Phytophthora,* and *Verticillium* etc. while species of *Pseudomonas, Ralstonia,* and *Xanthomonas* are the major bacterial phytopathogens which cause substantial yield losses to many important consumable crops [2]. And hence, to manage/control phytopathogens and consequently to optimize crop production, billions of dollars are invested in intensive agronomic practices. Among different strategies adopted by growers to protect plants from phyto-pathogenic damage vis-a-vis optimizing crop production includes, cultural practices for example, crop rotation, chemical control measures, and biological methods [3]. Use of pesticides among agrochemicals in contrast has been the most common practice to increase food security despite the fact that pesticides can have negative effects on consumers via food chain [4]. Recently, the use of pesticides has further increased due to its rapid impact and easy to apply approach compared to other pest control measures [5]. Chemicals used to control phytopathogens are however, considered unsafe when they are used beyond prescribed limits and are applied abruptly. However, none of the methods (cultural, chemical or biological) have been found completely successful in many cases. Moreover, the environmental hazards, toxic impact on useful soil microflora and emergence of resistance among pathogens against such chemicals are indeed some of the major global challenges which require immediate attention [6]. Apart from these, cost of pesticides and lack of appropriate application/delivery systems to resource-crunch farmers warrants the need for identifying alternate strategies to combat phytopathogens.

Due to these, agricultural scientists are searching for innocuous, inexpensive and sustainable options to trim down or to completely eliminate the use of pesticides including fungicides in agricultural practices and to battle out the emergence of resistance among fungal pathogens. In this context, the use of nanomaterials with precision and target specific activity has provided some solutions to the pesticide problems [7]. For example, silver nanoparticle (AgNP) has been found highly toxic to most pathogenic

microorganisms and therefore, may act as a suitable alternative for antimicrobials [8, 9]. As an example, Mahdizadeh et al. [10] have reported eco-friendly characteristics and strong antibacterial effects of different concentrations of silver nanoparticles against phytopathogenic fungi such as *Pythium aphanidermatum*, *Sclerotinia sclertiorum* and *Macrophomina phaseolina*.

Nanoparticles, however, when desired, can be generated by physical, chemical and biological methods. Of these, physico-chemical methods have certain disadvantages such as- (i) they are expensive (ii) require harmful organic chemicals and (iii) may cause environmental hazards [11]. In contrast, the biological methods involving microbes and plants have been found economical and are environmentally friendly [12]. Among plants, Neem (*Azadirachta indica*) found abundantly in India and in neighboring countries has long been used in the treatment of many diseases due to its medicinal properties [13]. Also, *A. indica* leaf extract has been used in the synthesis of various NPs like gold and zinc oxide [14, 15]. Considering the advantages of green synthesis and manifold activity of NPs, the present investigation was aimed at- (i) producing silver nanoparticles (AgNPs) using neem foliage (ii) characterization and yield optimization of AgNPs (iii) assaying morphology, mean particle diameter and crystalline size of AgNPs (iv) evaluating antimicrobial activity of AgNPs against phytopathogenic fungi belonging to genera *Penicillium* sp., *Fusarium* sp., and *Aspergillus* sp. and bacterium *Ralstonia solanacearum* and (v) measuring the cellular damage caused by AgNPs employing SEM. Indeed, the synthesis and antimicrobial effects of AgNPs on microorganisms other than those used in this study have been reported. Yet, we have added some new dimensions to furthering the understanding of the low cost green AgNPs and their consequential impact on both fungal and bacterial phytopathogens. Further, we have also explained as to how AgNPs forms agglomerates in solution. Other exciting features of the present study provides a base to better understand the mechanistic basis of successful pathogenesis including the leakage of DNA, loss of cellular metabolism, and surface adhering ability of bacterial/fungal pathogens.

Materials and Methods

Green Synthesis of *A. indica* Leaf Extract-AgNPs

Leaf extract of *A. indica* was prepared as described elsewhere [16]. The reaction mixture was prepared with aqueous *A. indica* leaf extract and 1 mM solution of silver nitrate ($AgNO_3$) at the ratio of 1:20. The reaction mixture was stirred rigorously at a speed of ≈ 450 rpm on a magnetic stirrer moving at ≈ 70 °C. The dark colored solution so developed was centrifuged at 10,000 rpm for 20 min. Supernatant was collected in a separate vial and respun at 10,000 rpm for 20 min. and the pellets were washed with DDW 3 times followed by drying in a vacuum oven for 12 h at 60 °C. Various reaction parameters such as molarity of $AgNO_3$ ranging from 0.2 to 1 mM, pH (5–9), and incubation time for AgNPs synthesis were optimized.

Characterization of AgNPs

Surface Plasmon Resonance (SPR), Crystal Size and Functional Groups of AgNPs

During synthesis, change in color from pale yellow to dark brown due to reduction of Ag^{2+} to Ag^0 was observed and increase in SPR was recorded by UV-Vis spectrophotometer [17]. To check the optimum synthesis of AgNPs, the UV-Vis spectra under varying experimental conditions such as pH, molar concentration of $AgNO_3$, and incubation periods were also recorded. Since, slightly alkaline conditions have been reported to accelerate the reduction of AgNPs [27], we also recorded the UV-Vis spectra (30–90 min.) at pH 8. The *A. indica* leaf extract mixed with DDW at the ratio of 1:20 was used as blank. The crystallinity, average size and functional groups of AgNPs was characterized by X-ray diffraction (XRD) and FTIR, respectively [17].

Morphology, Elemental Composition, Average Shape and Size of AgNPs

The morphology of AgNPs was determined by SEM equipped EDX [18] while the size and shape of AgNPs was determined by high resolution (HR) TEM (JEOL, Tokyo, Japan) [16]. The secondary size of AgNPs was also measured employing Dynamic Light Scattering (DLS) [16].

Isolation and Maintenance of Phyto-Pathogenic Fungi and Bacteria

The strains of *Penicillium* sp., *Aspergillus* sp., and *Fusarium* sp. were isolated from the diseased leaf surface and whole fruit of eggplant (*Solanum melongena*) grown at the Faculty of Agricultural Sciences, Aligarh Muslim University Aligarh, using standard procedures. These fungi were maintained on potato dextrose agar (PDA) supplemented with 50 μg ml^{-1} chloramphenicol. Sterile plates were then seeded with fungal spores (1.5 cm in diameter) at the center of petri dish followed by 10 days incubation at 28 °C. The bacterial pathogen *R. solanacearum* (NAIMCC-B-01626) was obtained from National Bureau

of Agriculturally Important Microorganisms (NBAIM), Kushmaur, U.P., India. The bacterium was sub-cultured in nutrient broth (NB) and maintained on nutrient agar slants and plates (1.8%).

Assay of Biocidal Activity of AgNPs

The antifungal activity of AgNPs was determined using semi-solid Rose Bengal Agar (RBA) culture medium treated with and without AgNPs. Overall, there were five treatments- (a) culture medium without AgNPs (control) and (b) medium with different concentrations (μg ml^{-1}) of AgNPs- (i) 50 (ii) 100 (iii) 200 and (iv) 400. To ensure homogeneity and reproducibility, 10 days old fungal cultures were used. A- 1.5 cm diameter smear of matured spores was used to warrant the existence of growth structures. The experiment was carried out in triplicate (n = 3) and each culture was grown for 2 days to ensure an adequate fungal growth and then photographs were taken at each interval. The photographs were then analyzed (ImageJ software) and the area of fungal growth in Petri dish were measured. Percent (%) inhibition of growth was determined using the following formula-

$$\% \text{ Inhibition} = \text{growth of control} - \text{growth of treatment}/\text{growth of control} \times 100$$

Similarly, antibacterial potential of AgNPs against *R. solanacearum* was analyzed by agar well diffusion method [17].

Determination of MIC and MBC of AgNPs Against *R. solanacearum*

Minimum inhibitory concentration (MIC) and minimum bactericidal concentration (MBC) of AgNPs against *R. solanacearum* were determined by growing bacterium in a NB medium supplemented with 6.25–400 μg mL^{-1} of AgNPs. After 24 h of growth, 100 μl from each treatment was spread on nutrient agar plates and grown for 24 h at 28 °C. The viable cells were counted after 24 h growth [17].

Time and AgNPs Concentration Dependent Growth of *R. solanacearum*

The survival ability of *R. solanacearum* in the presence of AgNPs was assessed by growing cells with 6.25, 12.5, 25, 50, 100, 200, and 400 μg ml^{-1} of AgNPs using a 96 well microtitre plate filled with 200 μl of NB followed by inoculation with 20 μl of young culture [17].

Measurement of Cellular Respiration of *R. solanacearum*

The cellular respiration of *R. solanacearum* under AgNPs stress was assessed using enzyme dehydrogenase assay [16]. Briefly, early log phase cells of *R. solanacearum* grown in NB were centrifuged (5000 rpm) for 10 min, and pellet was re-suspended in phosphate buffer (pH 7.0) to achieve an absorbance (Abs_{600}) of 0.4. A- 200 μl of suspension was added to each well of microtitre plate containing 0–400 μg ml^{-1} of AgNPs. Cell suspension without AgNPs served as control. To the cells of *R. solanacearum*, 40 μl of the probe 2, 3, 5-triphenyl-tetrazolium chloride (TTC) (0.5%, w/v) was added and allowed to incubate at room temperature. The change in color from colorless suspension to pink indicating positive reaction was instantly measured at 450 nm using microplate reader.

Determination of Nucleic Acid Leakage and Surface Adherence of *R. solanacearum* Under AgNPs Stress

The cells of *R. solanacearum* were grown in 100 ml capacity conical flasks containing 20 ml NB for overnight. The flasks except control were treated with 25, 50, 100, 200, and 400 μg ml^{-1} of AgNPs and incubated at 28 °C for 4 h on a rotatory shaker spun at 150 rpm. A-1.5 ml aliquot from each treatment was centrifuged at 5000 rpm for 5 min. A- 100 μl supernatant kept in a fresh tube was diluted with DDW (1.5 ml) and the spectra was recorded at 250–350 nm using UV-Vis spectrophotometer. The absorbance at 260 nm was separately plotted as a function of AgNPs concentration. The surface adhering ability of *R. solanacearum* under AgNPs (0–400 μg ml^{-1}), was determined using 20 μl of young bacterial culture (1×10^7 cfu ml^{-1}) in polystyrene microtitre wells containing 200 μl of NB and 6.25, 12.5, 25, 50, 100, 200, and 400 μg ml^{-1} of AgNPs. Wells were incubated at 28 °C for 24 h. Wells without AgNPs served as control. Further processing was done as described earlier [19].

Morphological Changes to Fungal and Bacterial Cells Under AgNPs Stress

Fungal strains of *Aspergillus* sp. and *Fusarium* sp. were grown on PDA in the absence and presence of 400 μg ml^{-1} AgNPs for 7 days. Afterward, a 1 cm^2 block having fungal growth was subsequently fixed in 2% paraformaldehyde and 2.5% gluteraldehyde in sterile tissue culture plate at 4 °C for 12 h. The fixed mycelia were washed three times with 1X PBS and then dehydrated by ethanol gradient (30-100%) for 10 min. each [17]. The block was then fixed on 18 × 18 mm glass cover slip by air drying and sputter coated with a 2 nm thin layer of gold. The samples were

visualized under SEM. Similarly, the morphological changes in *R. solanacearum* grown with 400 µg ml^{-1} of AgNPs for 12 h at 28 °C were detected by SEM.

Statistical analysis: Data represent the mean ± standard deviation (S.D.) of two independent experiments conducted in triplicate. Spectra were manually plotted and statistical analysis was performed by student's *t* test using SigmaPlot 12.0. Images were processed using ImageJ and Microsoft Powerpoint (2016) software.

Results

Visual Observation and Optimization of AgNPs Production

The first indicator of synthesis of AgNPs using *A.indica* leaf extract appeared within 90 min. in the form of pale yellow and then dark brown colored pigment (Fig. 1). The change in color from pale yellow to brown indicated a quick reduction of silver ions (Ag^{+}) to zerovalant silver (Ag^{0}) [17]. This difference in color could be considered as a primary evidence of reducing potential of *A. indica* leaf extract. The synthesis of AgNPs was further optimized by varying the reaction factors such as- (i) time (Fig. S1a), (ii) molarity of $AgNO_3$ (Fig. S1b), and (iii) pH (Fig. S1c). After optimization, the AgNPs were produced in bulk. Additionally, the AgNPs were further synthesized at room temperature (25 ± 2 °C) while other production conditions remained unchanged. Here, a delayed increase in SPR of AgNPs was observed. Therefore, use of low temperatures was avoided. Nucleation process of AgNPs was stopped after 90 min. and a peak maxima was achieved at λ = 437 nm. Absorption peak for *A. indica* leaf extract appeared at 334 nm which did not increase with increasing SPR of AgNPs in due course of time. The SPR of AgNPs at pH 8.0 was higher (Abs = 1.55 a.u.) than at pH 7 (Abs = 1.25 a.u.) and pH 9 (Abs = 1.46 a.u.).

Characterization of Green Synthesized AgNPs

Functional group analysis of A. indica leaf extract and AgNPs: The functional groups of *A. indica* leaf extract and AgNPs metabolites and their possible role in bioreduction of silver ions and stabilization of AgNPs as determined by FTIR was variable (Supplementary Table 1; Fig. S2a and Fig. S2b).

Crystal size of AgNPs: The XRD analysis revealed four characteristic planes of AgNPs in concurrence with Joint Committee on Powder Diffraction Standards (JCPDS) file No. 03–0921 of 2θ values from 20 to 80° (Fig. 2a). Signals in X-ray diffractogram of AgNPs at 37.16°, 43.1°, 63.8°, and 75.88° can well be assigned to 111, 200, 220 and 311 diffraction planes of face centered cubic (fcc) structure of silver which sufficiently revealed the crystal nature of AgNPs. The average crystal size of AgNPs calculated using full-width-at-half-maximum (FWHM) of 111 crystal plane was found as 21 nm.

Morphology and shape of AgNPs: The SEM micrographs of AgNPs demonstrated predominantly spherical nanoparticles which differed slightly in size (Fig. 2b, c). The HR-TEM images also showed spherical morphology of AgNPs (Fig. 2d). Mean particle diameter of AgNPs was observed as 29 ± 5 nm. The EDX spectra of AgNPs confirmed the presence of silver as weight percentage of 10.8 (Fig. S3). Besides Ag, peaks for O, C, Cl, Na, P, and K were also detected which might have been due to the capping of plant metabolites. The lattice fringe of AgNPs exhibiting the lattice *d* spacing of 0.23 nm in plane of AgNPs crystal are shown in Fig. 2e which is analogous to the fcc structure. The selected electron area diffraction (SAED) pattern of AgNPs revealed some diffraction planes as observed by intense diffraction dots which further validated the crystalline phase of AgNPs with a certain extent of polycrystallinity (Fig. 2f). Moreover, the diffraction spots in concentric rings of SAED can be well matched to the 311, 220, 200, and 111 planes of Ag detected in the XRD pattern (Fig. 2g). The secondary size of AgNPs measured by DLS was found to be 221 ± 12.4 nm due to particle agglomeration in aqueous dispersion (Fig. S4).

Antifungal Activity of AgNPs

The antimicrobial activity of newly synthesized AgNPs was assessed against both fungal (*Penicillium* sp., *Aspergillus* sp., *Fusarium* sp.) and bacterial (*R. solanacearum*) phytopathogens. The growth of *Aspergillus* (Fig. 3), *Fusarium* (Fig. 4) and *Penicillium* (Fig. 5) was significantly inhibited by varying concentrations of AgNPs which however, differed considerably with time. Also, there was no consistent relationship between fungal growth inhibition and incubation periods. The growth of *Aspergillus* was reduced maximally by 91% (after 2 days) which however reduced to 77% (after 4 days) and 69% (after 6 days) when grown in PDA medium treated with 400 µg AgNPs ml^{-1}. Similarly, the growth of *Fusarium* was reduced by 89% (after 2 days), 81% (after 4 days), and 89% (after 6 days) at 400 µg AgNPs ml^{-1} over untreated control. Likewise, a maximum of 57% (after 2 days), 62% (after 4 days), and 92% (after 6 days) reduction in mycelial growth of *Penicillium* was observed at 400 µg AgNPs ml^{-1}. From this finding it was evident that each concentration of AgNPs even-though had toxic impact on fungal growth but it was highest at 400 µgAgNPs ml^{-1} which almost completely inhibited the growth of fungal phytopathogens. The

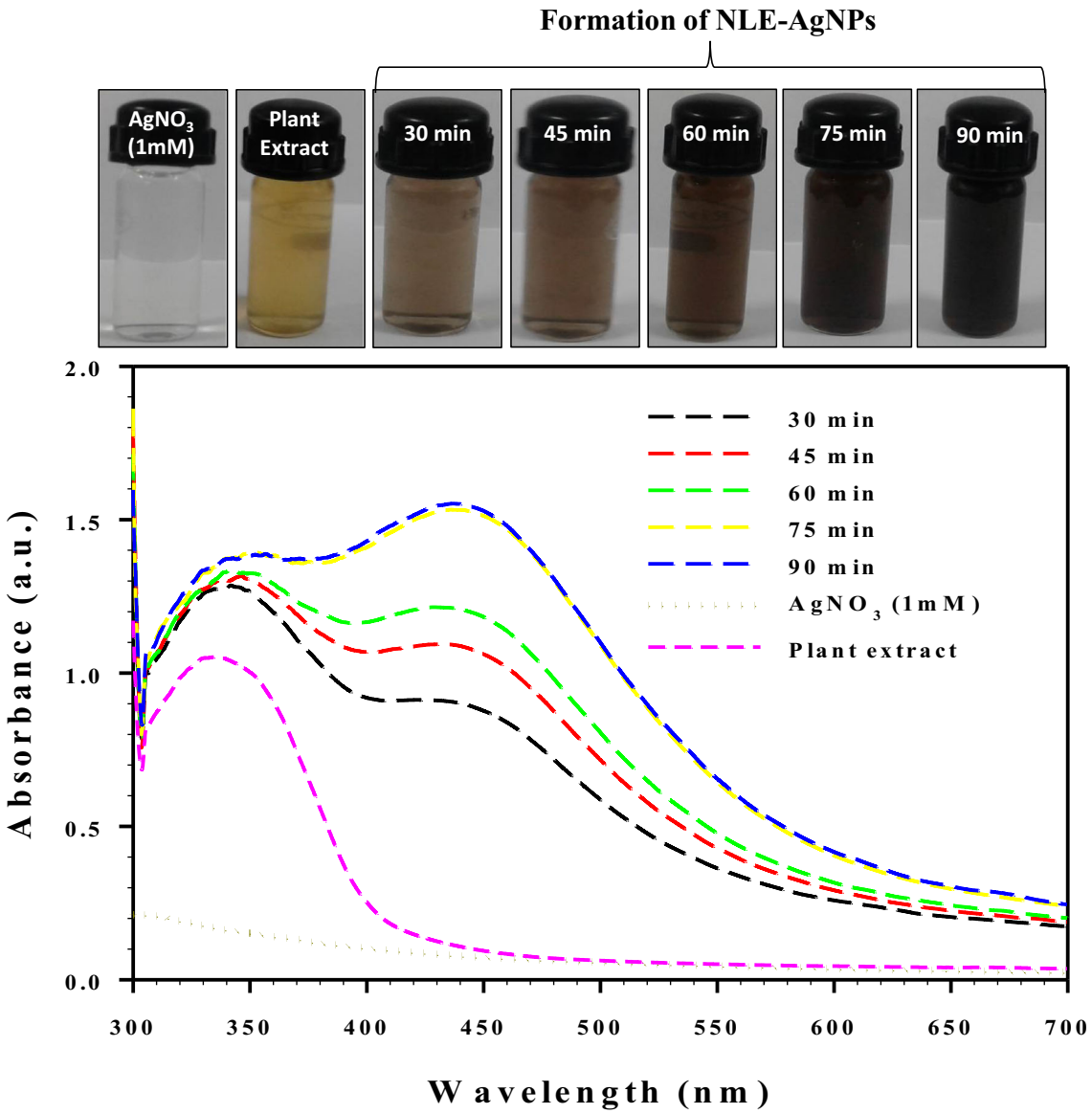

Fig. 1 UV-Visible spectra of AgNPs as a function of time (30–90 min.) with parallel control of plant extract and 1 mM $AgNO_3$ in a ratio of 1:20. The vials containing colored solutions of different intensities represent time dependent increase in SPR of AgNPs

sensitivity of AgNPs towards test fungi however followed the order: *Penicillium* > *Fusarium* > *Aspergillus*.

Morphological Analysis of Fungi Through SEM

The micromorphological images of *Penicillium* mycelia grown without AgNPs (Fig. S6 a–d) and with AgNPs (Fig. S6 e–h) differed substantially when viewed under SEM. The SEM image of untreated *Penicillium* mycelia (control) displayed normal hyphae with typical broom like appearance and smooth surface margin (Fig. S6 a–c). Also, the spores of *Penicillium* were intact without any visible surface distortion (Fig. S6 d). However, upon exposure to AgNPs, the mycelium lost its characteristic arrangement and surface smoothness (Fig. S6 e–f). Moreover, unusual pits were seen on the surface of mycelium (Fig. S6 g–h and g–h inset). Furthermore, the branching of conidia as observed in untreated control (Fig. S6 d) was not found in any of the region treated with AgNPs (Fig. S6 e). This finding further suggests that the development of conidia was also suppressed under AgNPs pressure. The spores were also deformed and contracted after exposure to 400 μg ml^{-1} AgNPs (Fig. S6 h inset). Similarly, the *Fusarium* was adversely affected by AgNPs (Fig. S7). The surface, structure, and spatial arrangement of mycelium and spores were normal without any deformity (Fig. S7 a–d), whereas, the mycelium treated with AgNPs was extensively destructed at various points (Fig. S7 a–d).

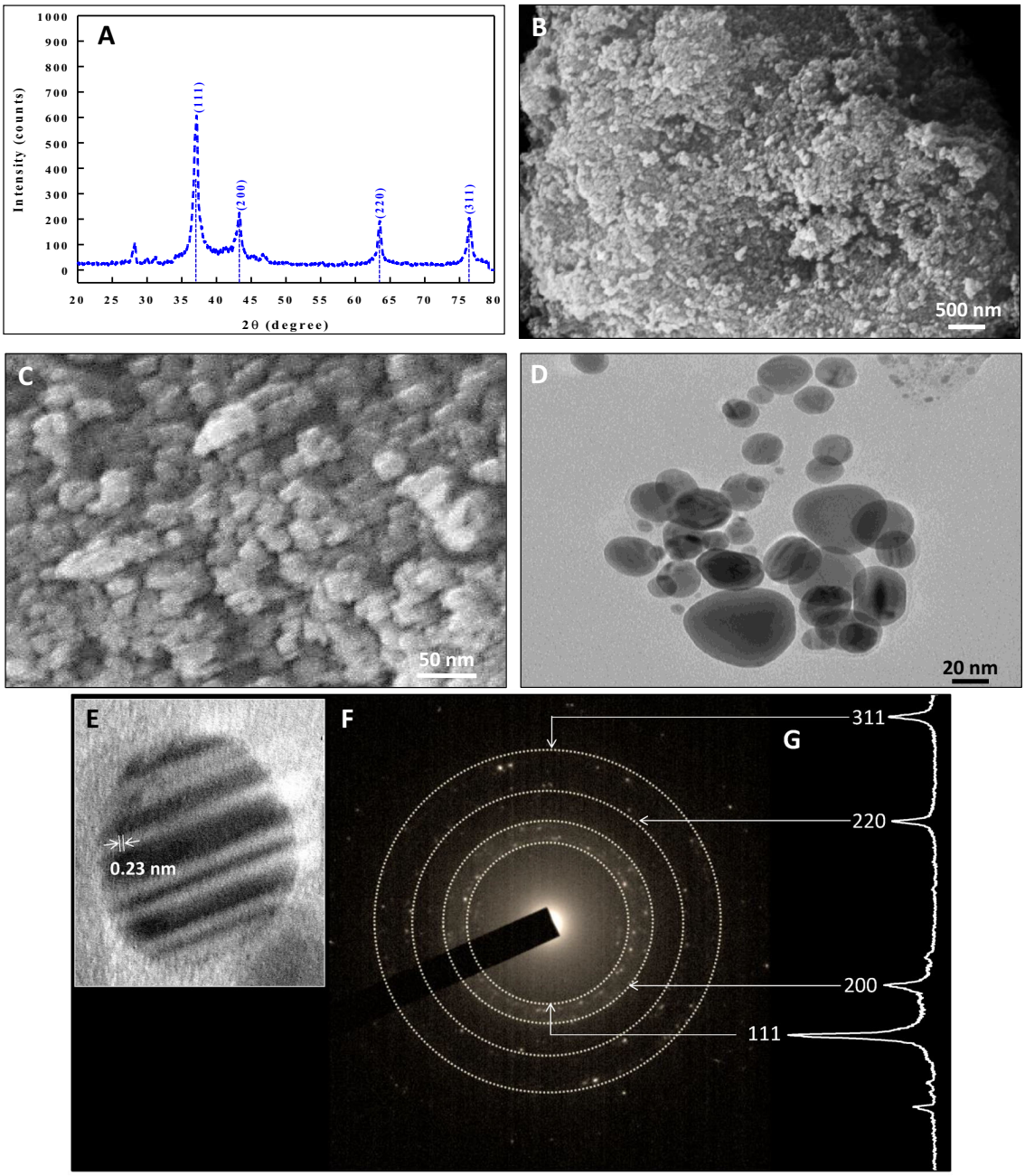

Fig. 2 X-ray diffractogram of AgNPs powder (panel A). Mean crystalline size through XRD was calculated as 21 nm. SEM of AgNPs (B and C) shows morphology of particle aggregates. TEM of AgNPs revealed the shape of individual *A. indica* leaf extract -AgNP with an average size of 29 ± 5 nm (Panel D). Lattice analysis of AgNPs by HR-TEM (Panel E) and SAED (Panel F). The peaks observed in XRD pattern (panel G) correspond to the concentric rings of electron dense spots in SAED pattern of AgNPs

Likewise, the shape and integrity of conidia were compromised under AgNPs (Fig. S7 d) and the changes were comparable to untreated control (Fig. S7 h).

Antibacterial Activity of AgNPs

Cellular respiration, surface adhering ability, nucleic acid discharge, time-concentration dependent growth measurements, and morphological changes in *R. solanacearum*

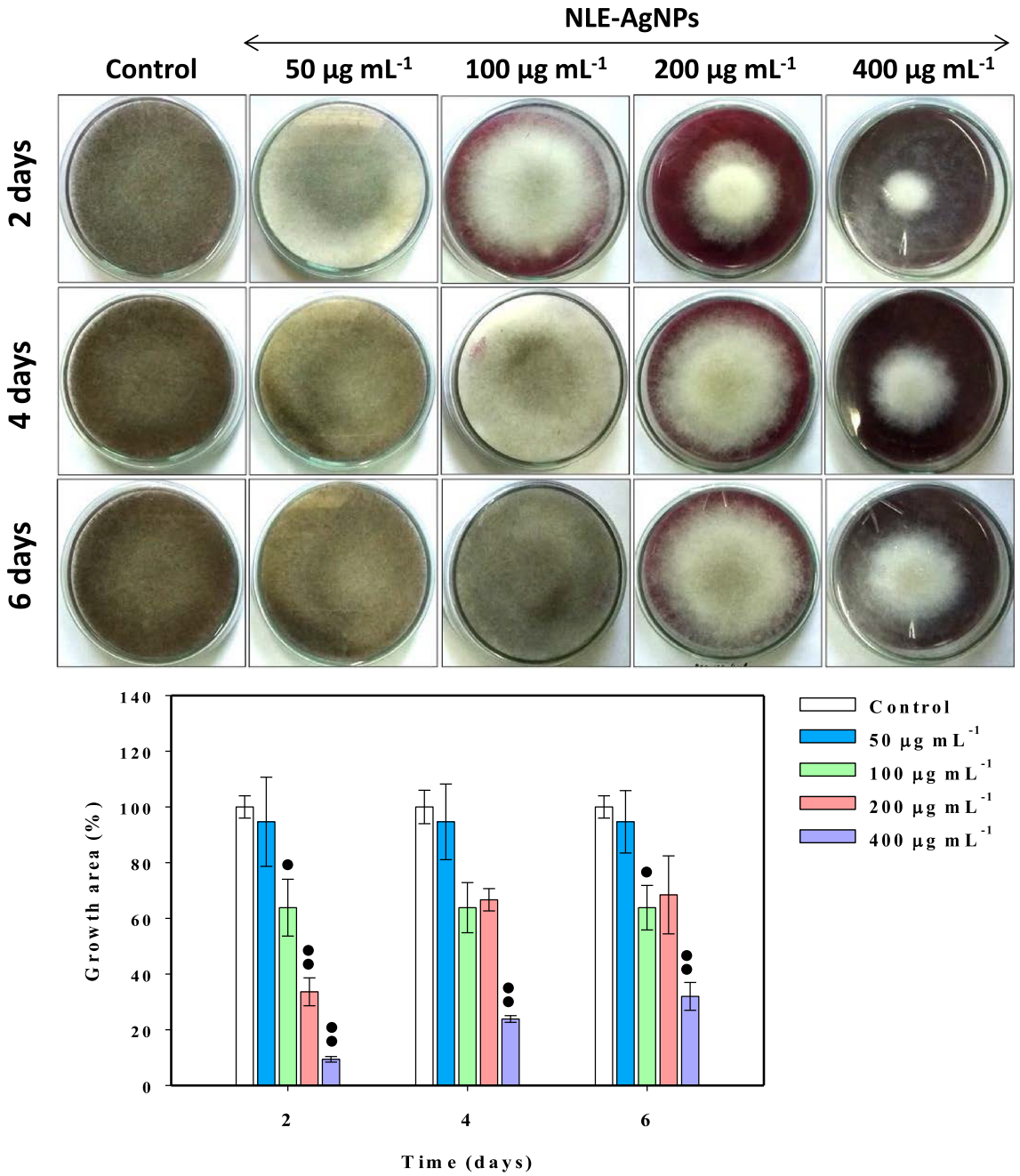

Fig. 3 Macroscopic examination of mycelial growth of *Aspergillus* sp. on medium supplemented with 50–400 µg ml-1 of AgNPs after 2, 4, and 6 days of growth. Bar diagram represents the numerical data in terms of percent growth area as compared to mycelial growth of untreated control. Values are mean ± S.D. of three replicates. Values of three replicates are expressed as mean ± S.D. (filled circle $P \leq 0.05$, two filled circle $P \leq 0.005$ vs. control)

established the growth inhibitory potential of all AgNPs. The MIC and MBC of AgNPs determined against bacterial pathogen was 200 and 400 µg ml^{-1}, respectively. The zone of growth inhibition increased with increasing concentrations of AgNPs (Fig. S5a). The zone of inhibition ranged between 13 mm (0.25 mg AgNPs/well) to 16 mm (1.5 mg AgNPs/well) as shown in Fig. S5b. Time kill bioassay of AgNPs against *R. solanacearum* at 6.25–400 µg ml^{-1} consolidated the facts that AgNPs hindered the bacterial growth (Fig. 6a). Bacterial growth stages including lag, log, and stationary were noticed under all treatment conditions. The growth of *R. solanacearum* exposed to the lower dose of AgNPs was also found marginally inferior versus control. At higher doses, AgNPs, inhibited the growth of test strain maximally which however was completely lost at 400 µg AgNPs ml^{-1}.

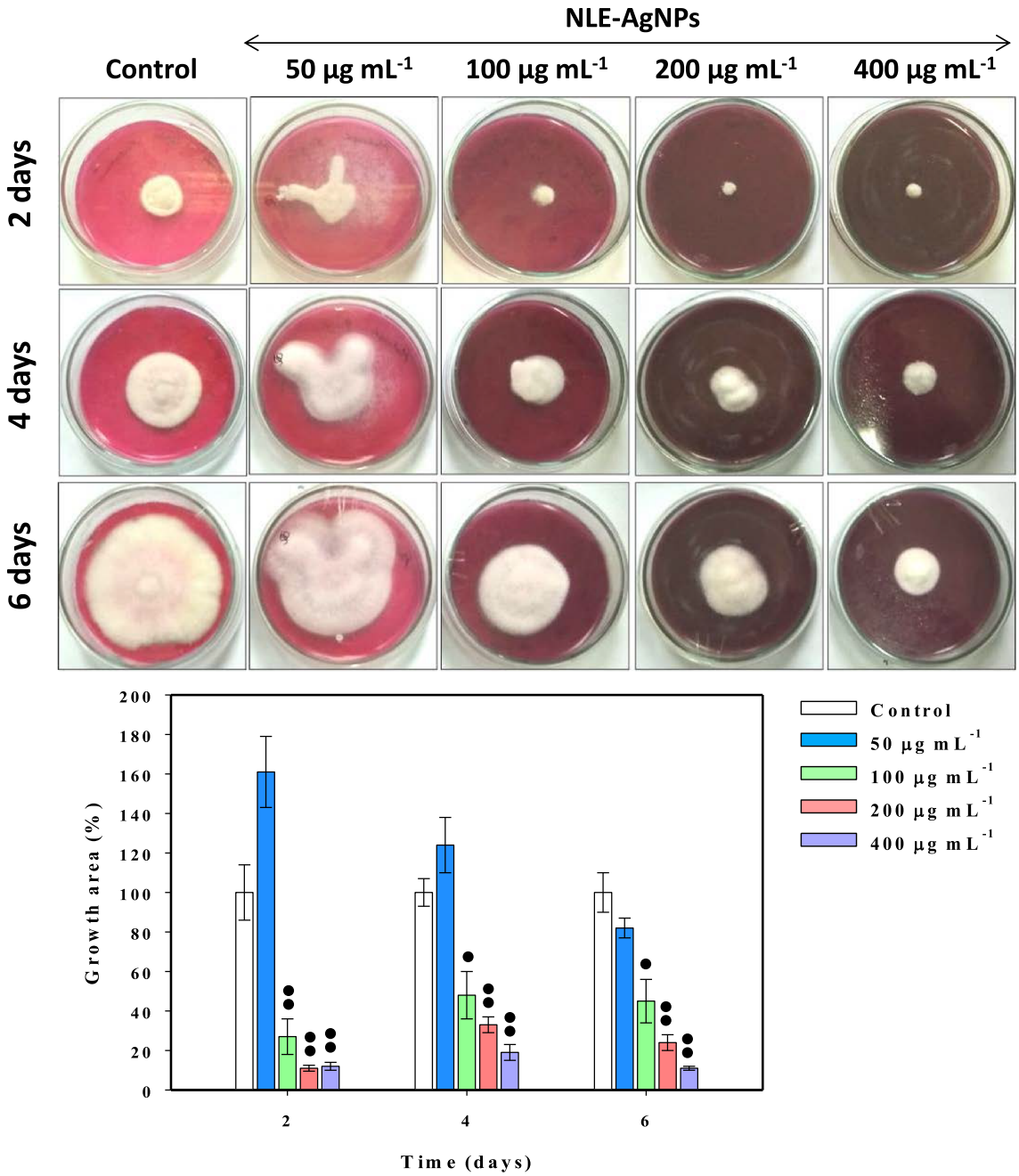

Fig. 4 Macroscopic examination of mycelial growth of *Fusarium* sp. on media supplemented with 50–400 µg ml-1 of AgNPs after 2, 4, and 6 days of growth. Bar diagram represents the numerical data in terms of percent growth area as compared to mycelial growth untreated control. Values are mean ± S.D. of three replicates. Values of three replicates are expressed as mean ± S.D. (filled circle $P \leq 0.05$, two filled circle $P \leq 0.005$ vs. control)

Morphology of *R. solanacearum* and Nucleic Acid Leakage Influenced by AgNPs

The SEM micrographs of untreated *R. solanacearum* cells was normal (Fig. 6b) while after exposure to AgNPs the cells exhibited extensive damage (Fig. 6c). The morphological characteristics such as surface and shape of cells grown without amendment of AgNPs were compact whereas the cells of *R. solanacearum* grown in the presence of AgNPs were distorted to the extent that none of the bacterial cells was intact and in good shape. Also, larger amount of pits, absence of cellular coverings at various places, gaps, fragments, and appearance of cell bulging were evident in AgNPs treated bacterial cells (Fig. 6c). Following the attachment, the generation of reactive oxygen species (ROS) may create some new pores in the

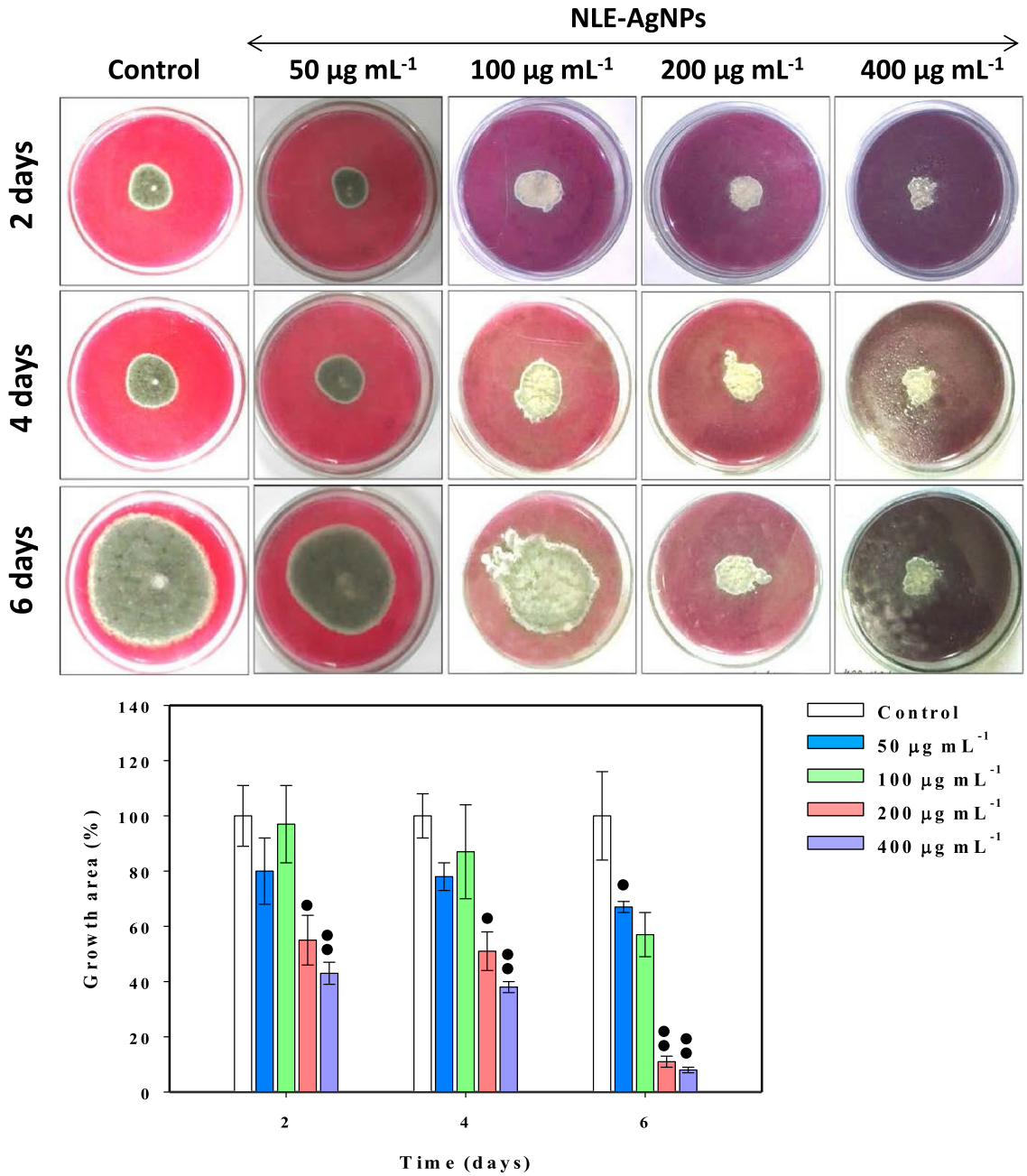

Fig. 5 Macroscopic examination of mycelial growth of *Penicillium* sp. on media supplemented with 50–400 µg ml-1 of AgNPs after 2, 4, and 6 days of age. Bar diagram represents the numerical data in terms of percent growth area as compared to mycelial growth untreated control. Values are mean ± S.D. of three replicates. Values of three replicates are expressed as mean ± S.D. (filled circle $P \leq 0.05$, two filled circle $P \leq 0.005$ vs. control)

cellular membranes of bacteria, and hence the discharge of cellular content including nucleic acids can predict the extent of membrane damage [17]. Therefore, experiments were performed to check the ability of AgNPs to knock out the nucleic acids through the altered cell membrane (Fig. 7a,b). The data of nucleic acid release exhibited dose dependent enhancement (8–34%) in the absorption at 260 nm which was found highest at 400 µg ml^{-1} after 5 h exposure (Fig. 7a). The enhanced nucleic acid discharge was maximum (34%) and highly significant ($r^2 = 0.97$) at 400 µg ml^{-1} AgNPs (Fig. 7b).

Surface Adherence and Cellular Respiration of *R. solanacearum* Under AgNPs Stress

The ability of *R. solanacearum* to adhere onto a solid surface such as polystyrene while growing with varying rates of AgNPs using crystal violet (CV) method differed

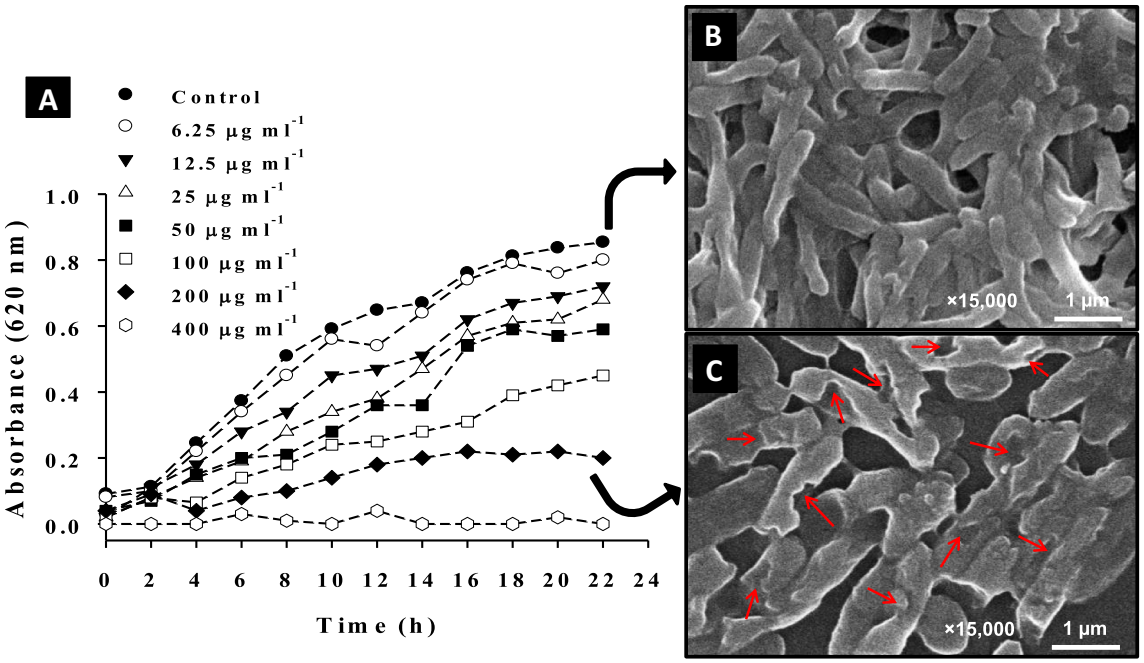

Fig. 6 Time (0–24 h) and concentration (0–400 µg ml^{-1}) dependent absorption (λ_{max} = 620 nm) spectra of *R. solanacearum* at various concentrations of ZnONPs (Panel A). Images of SEM at the magnification of × 15,000 in panel B (control cells) and C (cells treated with 200 µg ml^{-1} AgNPs) show the difference in cell morphology. Red arrows indicate damage or distortion (color figure online)

in a dose related fashion (Fig. 7c). Generally, each concentration of AgNPs reduced the adherence potential of *R. Solanacearum*. However, AgNPs at 400 µg ml^{-1} had maximum inhibitory impact on bacterial adherence ability. Compared to untreated control where the cells exhibited maximum retention of CV, the absorbance value measured from AgNPs treated cells decreased in the following order: 0.91 ± 0.2 (6.25 µg ml^{-1}), 0.8 ± 0.21 (12.5 µg ml^{-1}), 0.77 ± 0.29 (25 µg ml^{-1}), 0.55 ± 0.14 (50 µg ml^{-1}), 0.33 ± 0.05 (100 µg ml^{-1}) and 0.14 ± 0.01 (200 µg ml^{-1}). The AgNPs concentration dependent inhibition of respiration of *R. solanacearum* is presented in Fig. 7d. Inhibition of dehydrogenase activity was obvious and can be seen as a result of development of red formazan in untreated cells while with increasing concentrations of AgNPs (25–400 µg ml^{-1}), the reduction in cell metabolic activity was noticed. The percent decrease in absorbance (450 nm) over control was maximum (32%) at 25 µg ml^{-1} compared to other treatments.

Discussion

In order to optimize crop production, management of plant diseases caused by various phytopathogens is urgently required. To achieve this, variety of agrochemicals have been employed over a period of time. However, the uncontrolled use of agrochemicals despite lowering the outbreak of plant diseases, has also contributed to the emergence of resilient microbial pathogens [2]. Additionally, such chemicals destruct the rhizospheric microflora, beneficial insects, and indirectly affect food chain. Therefore, technologically advanced and innovative means are needed to address these issues. In this regard, nanotechnology as a promising alternative has provided solution to the problems. Although, some studies have explored the potential use of nano-based products in agriculture including pesticide degradation, fertilizers, micronutrients, soil remediation, nano-sensing of pesticides and pathogens, nevertheless, nanotechnology derived anti pathogenic agents remains largely unexplored [20, 21]. However, in some studies, metal based nanoparticles have been considered as an alternative to restrict the growth of various pathogenic microbes including fungi *Gloeophyllum abietinum* [22], *Chaetomium globosum* [22], *Phanerochaete sordida* [22], *Trichoderma harzianum* [10] and bacteria belonging to family Pseudomonadaceae, Xanthomonadaceae, and Enterobacteriaceae such as *Ralstonia solanacearum* [23]. Considering these, we focused on the green synthesis of metallic AgNPs and evaluation of its antifungal and antibacterial activity.

After the saturation of oxidized state of silver with electrons in reaction mixture within a few seconds accompanied by the small clusters formation, growth of AgNPs proceeded following the classical LaMer mechanism of growth [24]. It indicates that the metabolites of *A.*

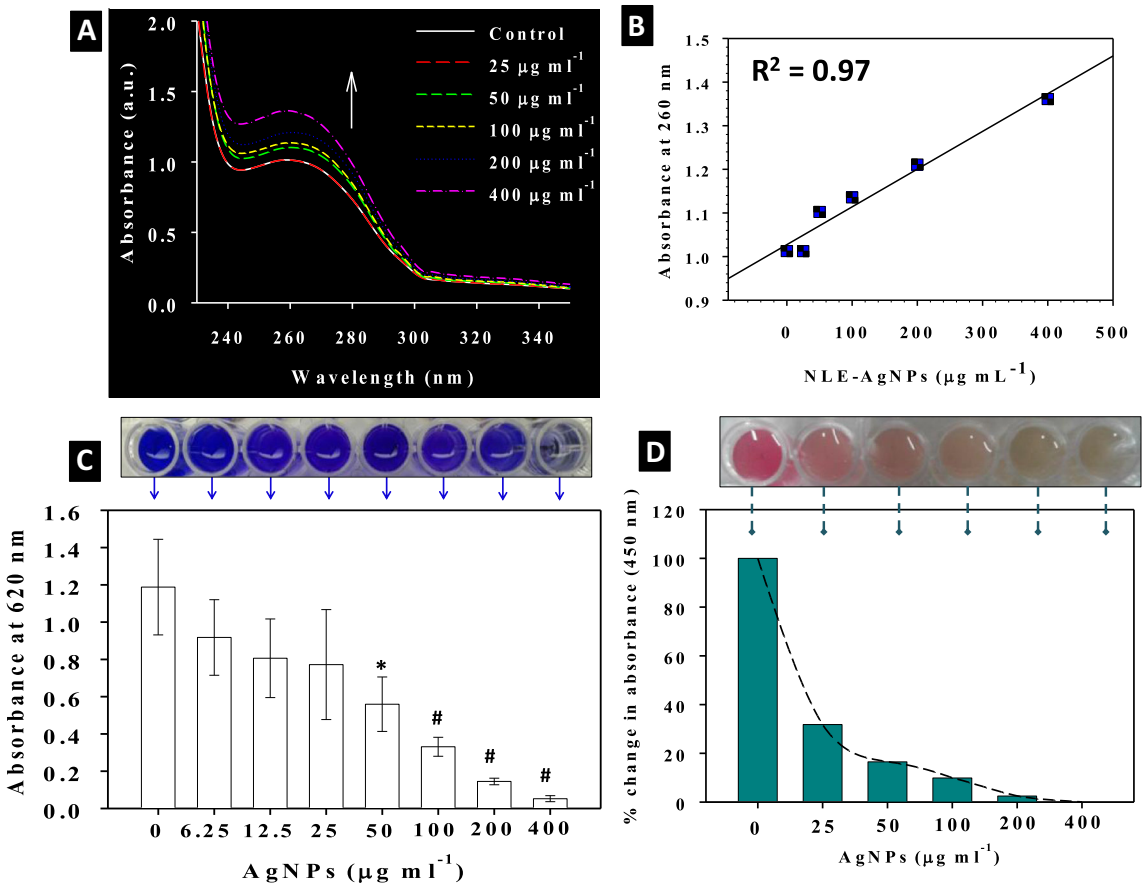

Fig. 7 Absorbance spectra (Panel A) of nucleic acid release from *R. solanacearum* after exposure with AgNPs. Panel B shows enhancement in optical density at 260 nm as a function of AgNPs concentration. Adherence of *R. solanacearum* on the surface of polystyrene wells (Panel C). Corresponding bar diagram represents the absorbance of crystal violet retained by bacterial cells after treating with 6.25–400 µg ml^{-1} AgNPs (Panel C). Inhibition of cellular respiration of *R. solanacearum* by AgNPs (Panel D). Intensity of resulting product formazan in microtitre plate wells represents metabolic activity of viable cells. Values of three replicates are expressed as mean ± S.D. (*$P \leq 0.05$, #$P \leq 0.005$ vs. control) (color figure online)

indica leaf extract were actively involved in reducing and stabilizing AgNPs. The absorption spectrum of AgNPs was nearly symmetrical with a broad absorption peak which is an indication of isotropism in AgNPs shape and size. Generally, the SPR is affected by shape, size, surface chemistry, and composition of nanoparticles [19]. Furthermore, the reduction of silver ions and formation of AgNPs by electron donating entities of leaf extract increased with increasing time at pH 8.0 and $AgNO_3$ molarity. The variation in SPR observed as a result of change in pH of reaction mixture could possibly be attributed to symmetric escalation of SPR in a time dependent fashion which is suggestive of inhibition of nanoparticles aggregation in reaction mixture. The higher SPR at pH 8.0 due to the smaller size of AgNPs was in agreement with the findings of *Maclura pomifera* leaf mediated synthesis of AgNPs at pH 8.0 [24]. The observations of green synthesis of AgNPs are in close agreement to the findings on AgNPs synthesized from extracts of *Cochlospermum religiosum* [25]. As data revealed, the higher yield of nanoparticles at slightly basic pH could be due to the oxidized leaf constituents with consequent release of electrons that instantly reduces silver ions [17]. The time for AgNPs synthesis was quite less to those reported by Ahmed et al. [26] who used one ml of *A. indica* leaf extract (24 h). The results further suggest that slightly basic pH could appreciably step up the rate of reaction and the yield of NPs. On the other hand, the formation of AgNPs even at higher pH was not completely abolished. The AgNPs remained stable at least for 8 weeks without any shift in peak absorption maxima. This stability could possibly be due to the capping of NPs by strong capping agents such as flavanones and terpenoids present in neem leaves [13, 14]. To substantiate this further, there are reports that plant based phenolic compounds consisting of flavonoids and polyphenols may coordinate with metal ions during nanoparticles synthesis [19].

The IR signals of *A. indica* leaf extract were also observed for AgNPs which explains the potential role of neem leaf organics in the synthesis of AgNPs. The broader signal for phenolics formed at distinctive spatial positions of phenolic compounds are expected to cause rapid reduction of silver ions by transfer of e^- resulting from electron deficiency in medium which is then maintained by resonating pie electrons (π-e^-) of the ring. The IR spectra of signal as reported by Chahardoli et al. [27] also confirmed the role of flavanones and phenolics of *Nigella arvensis* leaf extract in the reduction and capping of biogenic AgNPs. These shifts in wave numbers suggest the involvement of different functional moieties in capping and their absorption on the surface of AgNPs. On the basis of FT-IR results, it could be assumed that functional moieties of *A. indica* leaf extract which played a significant role in AgNPs synthesis included both aliphatic and aromatic ring structures that reduces silver ions and interacts with smaller AgNPs cluster and ultimately facilitates the capping of AgNPs.

The green synthesized AgNPs when tested for its antifungal activities showed prominent growth destruction of *Penicillum* sp., *Fusarium* sp., and *Aspergillus* sp. Similarly, antifungal potential of NPs has been documented by other scientists. For instance, He et al. [28] reported that ZnO-NPs inhibited the growth of *B. cinerea* and *P. expansum* by deforming the structure of fungal hyphae and halting the germination of conidia and conidial development. Additionally, the surface of fungal hyphae was deformed. Apart from these, the AgNPs also disrupt membrane transport systems including ion efflux. The distorted membranes may allow the accumulation of silver ions released from AgNPs in the nutrient media which in effect alters cellular respiration and metabolic activities [29]. Generation of intracellular ROS is yet another mechanism by which the lipids, proteins, and nucleic acids are adversely influenced [17]. The green synthesized AgNPs exhibited strong antibacterial activity and inhibited the growth of *R. solanacearum*. This finding is quite interesting from agronomic point of view for the reason that *R. solanacearum* among bacterial pathogens cause significant losses to crop production [24]. For instance, the deadly wilting disease caused by *R. solanacearum* affects various agricultural crops such as tomato and tobacco [23]. And hence, some of the promising traditional strategies adopted to mitigate the adverse effects of *R. solanacearum* have been the breeding of resistant species, cultural practices and crop rotation [30]. However, the efficacy of such practices has been found highly variable. Therefore, the antibacterial action of AgNPs as observed in this study could be vital in containing the bacterial phytopathogens [29]. Mechanistically, strong interactions of AgNPs with the cell wall influence the high surface energy and mobility of nanoparticles [29]. Also, the negatively charged LPS layer of *R. solanacearum* make it more sensitive to AgNPs action which may alter membrane transport resulting in increased cell permeability leading to the leakage of cell content including nucleic acids and ultimately causing cell death [19, 29]. Additionally, the swift attachment of AgNPs on bacterial surface enhances ROS production and release of other superoxides increasing the porosity of cell membranes which in turn paves the way for nucleic acid discharge from the cell [31].

Apart from these, the soil borne pathogen *R. solanacearum* invades crop through injured roots and spreads through vascular system of host plants employing its adherence and colonizing efficiency [23]. To establish adherence and colonization potential, bacterial cells were grown with AgNPs. Due to their non-specific targets, AgNPs are expected to inhibit the metabolism of bacteria involved in extracellular polymeric substance (EPS) production which mainly comprises of polysaccharides with secreted proteins [17]. The inhibition of cellular respiration by AgNPs has also been described with some other NPs in Gram negative species of *E. coli*, *P. aeruginosa*, and nitrifying bacteria [16]. It has been speculated that interaction of NPs with cell membrane components cause inhibition of respiration. The results obtained here validate the findings on surface adherence and growth inhibition as discussed earlier.

It can be concluded that the need of effective nanopesticides which can be synthesized using natural metabolites of plants is of paramount importance to avoid/reduce the use of harmful synthetic chemicals. In this work, we compared and discussed the antifungal and antibacterial action of stabilized AgNPs against *Penicillium* sp., *Aspergillus* sp., *Fusarium* sp., and *R. solanacearum* which limits the performance of agronomically important crops. The AgNPs synthesized here has shown both fungicidal and bactericidal activity. The AgNPs solution at various concentrations also exhibited significant anti-adherence activity, metabolic passiveness, compromised membrane integrity, and time dependent killing of *R. solanacearum*. Moreover, the micromorphological features of both fungal hyphae and bacterial cells were altered, when grown in the presence of AgNPs. Results obtained in this study therefore, suggests that such AgNPs as synthesized here, possessing enough anti-pathogenic potential could safely and efficiently be used as an alternative to chemical control strategies employed to manage the phytopathogens capable of causing losses to in agriculture production in different agro-ecological niches.

Acknowledgments Mohammad Saghir Khan, Bilal Ahmed, and Javed Musarrat acknowledge the Council of Science and Technology, U.P., India for the financial support through the Research Grant #372.

Mr. Pramod Kumar Sahu, Scientist, NBAIM, Mau, India is greatly acknowledged for providing the strain of *R. solanacearum* (NAIMCC-B-01626). The authors are also thankful for the support extended by University Sophisticated Instruments Facility (USIF), Aligarh Muslim University, Aligarh, India.

Compliance with Ethical Standards

Conflict of interest The authors declare that there are no conflicts of interest.

References

1. Katan J (2017) Diseases caused by soilborne pathogens: biology, management and challenges. J Plant Pathol 99:305–315. https://doi.org/10.4454/jpp.v99i2.3862
2. Shahid M, Zaidi A, Khan MS, Rizvi A, Saif S, Ahmed B (2017) Recent advances in management strategies of vegetable diseases. In: Microbial strategies for vegetable production, pp 197–226. https://doi.org/10.1007/978-3-319-54401-4_9
3. Al-Mughrabi KI, Vikram A, Poirier R, Jayasuriya K, Moreau G (2016) Management of common scab of potato in the field using biopesticides, fungicides, soil additives, or soil fumigants. Biocontrol Sci Technol 26:125–135. https://doi.org/10.1080/09583157.2015.1079809
4. Damalas CA, Eleftherohorinos IG (2011) Pesticide exposure, safety issues, and risk assessment indicators. Int J Environ Res Public Health 8:1402–1419. https://doi.org/10.3390/ijerph8051402
5. Shahid M, Ahmed B, Khan MS (2018) Evaluation of microbiological management strategy of herbicide toxicity to greengram plants. Biocatal Agric Biotechnol 14:96–108. https://doi.org/10.1016/j.bcab.2018.02.009
6. Shahid M, Ahmed B, Zaidi A, Khan MS (2018) Toxicity of fungicides to: pisum sativum: a study of oxidative damage, growth suppression, cellular death and morpho-anatomical changes. RSC Adv 8:38483–38498. https://doi.org/10.1039/c8ra03923b
7. Bahrami-Teimoori B, Nikparast Y, Hojatianfar M, Akhlaghi M, Ghorbani R, Pourianfar HR (2017) Characterisation and antifungal activity of silver nanoparticles biologically synthesised by *Amaranthus retroflexus* leaf extract. J Exp Nanosci 12:129–139. https://doi.org/10.1080/17458080.2017.1279355
8. Sandeep K, Lee J-K, Singh GP, Singh M, Bhatia SK, Kalia VC, Patel SKS (2019) Biotechnological application of polyhydroxyalkanoates and their composites as anti-microbials agents. In: Biotechnological applications of polyhydroxyalkanoates. Springer, Singapore, pp 207–225. https://doi.org/10.1007/978-981-13-3759-8_8
9. Otari SV, Pawar SH, Patel SKS, Singh RK, Kim SY, Lee JH, Zhang L, Lee JK (2017) *Canna edulis* leaf extract-mediated preparation of stabilized silver nanoparticles: characterization, antimicrobial activity, and toxicity studies. J Microbiol Biotechnol 27:731–738. https://doi.org/10.4014/jmb.1610.10019
10. Mahdizadeh V, Safaie N, Khelghatibana F (2015) Evaluation of antifungal activity of silver nanoparticles against some phytopathogenic fungi and *Trichoderma harzianum*. J Crop Prot 4:291–300
11. Ahmed B, Dwivedi S, Abdin MZ, Azam A, Al-Shaeri M, Khan MS, Saquib Q, Al-Khedhairy AA, Musarrat J (2017) Mitochondrial and chromosomal damage induced by oxidative stress in Zn^{2+} ions, ZnO-Bulk and ZnO-NPs treated *Allium cepa* roots. Sci Rep. https://doi.org/10.1038/srep40685
12. Kalia VC, Patel SKS, Kang YC, Lee JK (2019) Quorum sensing inhibitors as antipathogens: biotechnological applications. Biotechnol Adv 37:68–90. https://doi.org/10.1016/j.biotechadv.2018.11.006
13. Sonalkar MY, Nitave SA, Kagalkar AA (2014) Review on neem plant. World J Pharm Pharm Sci 3:590–598
14. Bindhani BK, Panigrahi AK (2014) Green synthesis of gold nanoparticles using neem (*Azadirachta indica* L.) leaf extract and its biomedical applications. Int J Adv Biotechnol Res 5:457–464
15. Elumalai K, Velmurugan S (2015) Green synthesis, characterization and antimicrobial activities of zinc oxide nanoparticles from the leaf extract of *Azadirachta indica* (L.). Appl Surf Sci 345:329–336. https://doi.org/10.1016/j.apsusc.2015.03.176
16. Solanki B, Khan MS, Ahmed B, Musarrat J, Zaidi A (2018) Bacterial toxicity of biomimetic green zinc oxide nanoantibiotic: insights into ZnONP uptake and nanocolloid–bacteria interface. Toxicol Res (Camb) 8:246–261. https://doi.org/10.1039/c8tx00267c
17. Ahmed B, Hashmi A, Khan MS, Musarrat J (2018) ROS mediated destruction of cell membrane, growth and biofilms of human bacterial pathogens by stable metallic AgNPs functionalized from bell pepper extract and quercetin. Adv Powder Technol 29:1601–1616. https://doi.org/10.1016/j.apt.2018.03.025
18. Ahmed B, Khan MS, Musarrat J (2018) Toxicity assessment of metal oxide nano-pollutants on tomato (*Solanum lycopersicon*): a study on growth dynamics and plant cell death. Environ Pollut 240:802–816. https://doi.org/10.1016/j.envpol.2018.05.015
19. Saleem S, Ahmed B, Khan MS, Al-Shaeri M, Musarrat J (2017) Inhibition of growth and biofilm formation of clinical bacterial isolates by NiO nanoparticles synthesized from *Eucalyptus globulus* plants. Microb Pathog 111:375–387. https://doi.org/10.1016/j.micpath.2017.09.019
20. Singh S, Singh BK, Yadav SM, Gupta AK (2015) Applications of nanotechnology in agricultural and their role in disease management. Res J Nanosci Nanotechnol 5:1–5. https://doi.org/10.3923/rjnn.2015.1.5
21. Patel SKS, Kim JH, Kalia VC, Lee JK (2019) Antimicrobial activity of amino-derivatized cationic polysaccharides. Indian J Microbiol 59:96–99. https://doi.org/10.1007/s12088-018-0764-7
22. Narayanan KB, Park HH (2014) Antifungal activity of silver nanoparticles synthesized using turnip leaf extract (*Brassica rapa* L.) against wood rotting pathogens. Eur J Plant Pathol 140:185–192. https://doi.org/10.1007/s10658-014-0399-4
23. Chen J, Li S, Luo J, Wang R, Ding W (2016) Enhancement of the antibacterial activity of silver nanoparticles against phytopathogenic bacterium *Ralstonia solanacearum* by stabilization. J Nanomater. https://doi.org/10.1155/2016/7135852
24. Azizian-Shermeh O, Einali A, Ghasemi A (2017) Rapid biologically one-step synthesis of stable bioactive silver nanoparticles using Osage orange (*Maclura pomifera*) leaf extract and their antimicrobial activities. Adv Powder Technol 28:3164–3171. https://doi.org/10.1016/j.apt.2017.10.001
25. Sasikala A, Linga Rao M, Savithramma N, Prasad TNVKV (2015) Synthesis of silver nanoparticles from stem bark of *Cochlospermum religiosum* (L.) Alston: an important medicinal plant and evaluation of their antimicrobial efficacy. Appl Nanosci 5:827–835. https://doi.org/10.1007/s13204-014-0380-8
26. Ahmed S, Ullah S, Ahmad M, Swami BL, Ikram S (2015) Green synthesis of silver nanoparticles using *Azadirachta indica* aqueous leaf extract. J Radiat Res Appl Sci 9:1–7. https://doi.org/10.1016/j.jrras.2015.06.006
27. Chahardoli A, Karimi N, Fattahi A (2018) *Nigella arvensis* leaf extract mediated green synthesis of silver nanoparticles: their characteristic properties and biological efficacy. Adv Powder Technol 29:202–210. https://doi.org/10.1016/j.apt.2017.11.003

28. He L, Liu Y, Mustapha A, Lin M (2011) Antifungal activity of zinc oxide nanoparticles against *Botrytis cinerea* and *Penicillium expansum*. Microbiol Res 166:207–215. https://doi.org/10.1016/j.micres.2010.03.003
29. Dakal TC, Kumar A, Majumdar RS, Yadav V (2016) Mechanistic basis of antimicrobial actions of silver nanoparticles. Front Microbiol. https://doi.org/10.3389/fmicb.2016.01831
30. Zhao Y, Zhang C, Chen H, Yuan M, Nipper R, Prakash CS, Zhuang W, He G (2016) QTL mapping for bacterial wilt resistance in peanut (*Arachis hypogaea* L.). Mol Breed 36:1–11. https://doi.org/10.1007/s11032-015-0432-0
31. Onodera A, Nishiumi F, Kakiguchi K, Tanaka A, Tanabe N, Honma A, Yayama K, Yoshioka Y, Nakahira K, Yonemura S, Yanagihara I, Tsutsumi Y, Kawai Y (2015) Short-term changes in intracellular ROS localisation after the silver nanoparticles exposure depending on particle size. Toxicol Rep 2:574–579. https://doi.org/10.1016/j.toxrep.2015.03.004